Acta Ophthalmologica

Loss of retinal tension and permanent decrease in retinal function: a new porcine model of rhegmatogenous retinal detachment

Nina Buus Sørensen,[1] Anders Tolstrup Christiansen,[1] Troels Wesenberg Kjær,[2] Kristian Klemp,[1] Morten la Cour,[3] Steffen Heegaard,[3,4] Karin Warfvinge[5] and Jens Folke Kiilgaard[1]

[1]Department of Ophthalmology, Copenhagen University Hospital, Rigshospitalet, Copenhagen, Denmark
[2]Department of Neurology, Zealand University Hospital, Roskilde, Denmark
[3]Department of Ophthalmology, Copenhagen University Hospital, Rigshospitalet, Glostrup, Denmark
[4]Department of Pathology, Copenhagen University Hospital, Rigshospitalet, Copenhagen, Denmark
[5]Department of Clinical Experimental Research, Glostrup Research Institute, Rigshospitalet, Glostrup, Denmark

ABSTRACT.

Purpose: **Permanent loss of visual function after rhegmatogenous retinal detachment can occur despite successful surgical reattachment in humans. New treatment modalities could be explored in a detachment model with loss of retinal function. In previous porcine models, retinal function has returned after reattachment, regardless of height and duration of detachment. Difference in retinal tension between the models and the disease might explain these different outcomes. This study investigates, for the first time in an *in vivo* porcine model, another characteristic of rhegmatogenous retinal detachment – the loss of retinal tension.**

Methods: **Left eyes (n = 12) of 3-month-old domestic pigs were included. Baseline multifocal electroretinogram (mfERG) and a fundus photograph were obtained following anaesthesia (isoflurane). The pigs were vitrectomized, saline was injected subretinally, and the RPE was removed. The eyes were evaluated at 2, 4 and 6 weeks after surgery. Four eyes were enucleated at each evaluation for histologic examinations.**

Results: **A retinal detachment structurally resembling rhegmatogenous retinal detachment was induced in 11 out of 12 pigs. MfERG amplitudes were significantly decreased despite partial reattachment four and 6 weeks after detachment. The retinal thickness decreased with 27%, the inner nuclear layer degenerated, Müller cells hypertrophied, and outer segments were lost. In the ganglion cell layer, cellularity increased and there was cytoplasmic staining with Cyclin D1. Vimentin and GFAP staining for glial cells increased. After 2 weeks of detachment, the ganglion cells had lost their nucleus and nucleolus.**

Conclusions: **Loss of retinal tension in the detached retina seems to induce permanent damage with loss of retinal function. Death of ganglion cells, observed as soon as 2 weeks after detachment, explains the permanent loss of retinal function. The new model enables investigations of time-relationship between retinal detachment and lasting damage in addition to exploration of novel treatment modalities.**

Key words: animal model – intermediate filaments – mammal – Neuroprotection – retinal surgery – RPE damage – subretinal surgery

Acta Ophthalmol. 2020: 98: 145–152

doi: 10.1111/aos.14188

Introduction

Permanent visual damage occurs shortly after rhegmatogenous retinal detachment (Pastor et al. 2016). This contrasts to serous retinal detachments where vision is preserved for a prolonged time (Nicholson et al. 2013). In both types of retinal detachment, the photoreceptors are separated from the RPE, and the functional outcome must therefore be determined by another factor.

Retinal tension might be one of the determining factors for functional outcome after detachment. A main characteristic of rhegmatogenous retinal detachment, besides separation of photoreceptors and RPE, is loss of retinal tension. Contrary, in a serous retinal detachment, the retinal tension is maintained.

In previous models of rhegmatogenous retinal detachment in different species, fluid has been injected into the subretinal space (Anderson et al. 1983, 1986; Erickson et al. 1983; Guerin et al. 1989, 1990, 1993; Fisher et al. 1991, 2001, 2005; Cook et al. 1995; Lewis et al. 1998, 2002, 2005; Jacobs et al. 2002; Lewis & Fisher 2003; Linberg et al. 2009; Mandal et al. 2011; Sorensen et al. 2012, 2017b). These models have allowed examination of retinal function after separation of RPE and photoreceptors by "vitreoretinal fluid", which is one aspect of rhegmatogenous retinal detachment. Proper anatomical apposition between the RPE and photoreceptors is

considered crucial for retinal function (Sparrow et al. 2010). However, contrary to the loss of retinal tension seen in rhegmatogenous retinal detachments, the injection of subretinal fluid produces a retinal detachment with increased retinal tension.

Increased retinal tension has been shown, *in vitro*, to protect the porcine retina against damage (Taylor et al. 2013). These protective mechanisms induced by increased retinal tension could explain our earlier findings in porcine models. After injection of subretinal fluid, we have previously shown that: (1) A prolonged shallow retinal detachment induced by subretinal injection of Healon is well tolerated for 6 weeks (Sorensen et al. 2012) and (2) A tall separation of the photoreceptors from the RPE by decalin is well tolerated for at least 2 weeks (Sorensen et al. 2017b).

These findings contrast with the permanent loss of retinal function observed shortly after rhegmatogenous retinal detachment in humans (Pastor et al. 2016). A new *in vivo* animal model of retinal detachment with loss of retinal tension could therefore provide new knowledge on determining factors for retinal function.

Extensive removal of RPE could be a method to surgically induce a retinal detachment with loss of retinal tension. Water is constantly produced in the subretinal space, as a result of the high retinal metabolism and the intraocular pressure (Hamann 2002; Strauss 2005). One of the mechanisms that keeps the retina attached is the negative pressure created by the constant removal of this water from the subretinal space by the RPE (Strauss 2005).

RPE debridement in itself does not permanently damage retinal function (Sorensen et al. 2013). In previous studies, we have shown that:
1 RPE proliferating from the periphery covers denuded Bruch's membrane (Kiilgaard et al. 2007) and
2 Retinal function returns when proliferating RPE covers the lesion (Sorensen et al. 2013).

Removal of RPE could therefore be a new method to induce a retinal detachment without the increased retinal tension created by injection of subretinal fluid.

This paper presents a new surgical model of retinal detachment with loss of retinal tension, structurally resembling rhegmatogenous retinal detachment. The effect of the detachment was evaluated morphologically using histology and examined functionally using multifocal electroretinography (mfERG).

Material and Methods

Left eyes (n = 12) from domestic pigs of a Danish Landrace/Duroc/Hampshire/Yorkshire breed were included in the study. All pigs weighed approximately 25 kg at inclusion. In addition, one pig which had completed a gastrosurgical experiment was enucleated for baseline histology. The remaining 12 pigs underwent RPE debridement and were evaluated at 2 (n = 12), 4 (n = 8) and 6 weeks (n = 4) after surgery. Four pigs were sacrificed for histological analysis at each evaluation time point. The first pig that underwent surgery did not experience a retinal detachment, and it has been excluded. Surgery and evaluations were performed under general anaesthesia. The research protocol complied with the ARVO statement on the use of animals in ophthalmic and vision research and was approved by the Danish Animal Experiments Inspectorate (permission number 2012-15-2934-00151). A veterinarian supervised all animal procedures.

Anaesthesia and surgery

All animals were fasted for 18 hr prior to anaesthesia but had free access to water. Zoletil 50 Vet (containing 1.19 mg/kg of both tiletamine and zolazepam; Virbac SA, Carros, France) was used for preanaesthesia. Pupils were dilated to >8 mm using a combination of topical 0.4% benoxinate hydrochloride (oxybuprocaine; Amgros, Copenhagen, Denmark), 10% phenylephrine hydrochloride (metaoxedrine chloride; Amgros), 0.5% tropicamide (Mydriacyl; Alcon, Hainaut, Belgium) and 1% atropine sulphate (Amgros). The pigs were endotracheally intubated and anaesthetized with 2.5%–3.0% isoflurane (Attane vet; ScanVet Animal Health A/S, Fredensborg, Denmark) administered with 0.5 L/min 100% oxygen and 2.5 L/min humidified atmospheric air. The stroke volume (10 mL/kg) and respiratory frequency (16/min) were kept constant. The pigs were hydrated with isotonic NaCl intravenously (IV) (9 mg/mL; Fresenius Kabi, Bad Homburg, Germany), and body temperature was maintained at 38–39°C. Heart rate, ECG, carbon dioxide tension and oxygen saturation levels were monitored. In the anaesthetized animals, three sclerotomies were obtained at 10, 2 and 5 o'clock, 2 mm posterior to the corneal limbus. After securing an infusion line with Ringer Lactate (SAD, Copenhagen, Denmark), a standard three-port core vitrectomy and removal of the posterior hyaloid were performed using a 21 G vitrector (Karl Storz GmbH, Tuttlingen, Germany). A retinal bleb was produced by manual subretinal injection of a balanced salt solution (BSS PLUS, Alcon, Texas, USA) through a 41G cannula. A peripheral retinotomy was made in the bleb, and a 23G curved membrane peeler (Curved membrane scraper, DSP, Alcon, Copenhagen, Denmark) was introduced to obtain RPE debridement in an area equal to the size of two optic discs. There were no infections, intravitreal haemorrhage, or other serious complications after surgery in the 12 pigs.

MfERGs and fundus photography

Multifocal electroretinogram (mfERG) were recorded at baseline and at the evaluation time points, 15 min after the induction of anaesthesia. A global flash stimulation protocol (one standard frame, one full-field dark frame, one full-field flash frame and one full-field dark frame) with a black-and-white 103 unscaled hexagon stimulus array was used (Shimada et al. 2005). The frame refresh rate was 75 Hz with an m-sequence exponent of 12, which resulted in a 3-min and 38-second recording (Sorensen et al. 2017a). The mfERG settings were described previously (Sorensen et al. 2013). MfERGs were recorded in an electrically shielded room using a VERIS multifocal system with VERIS 6.0.8 software (EDI, Inc., Redwood, USA). The animals and the respirator were electrically grounded. A Burian-Allen bipolar adult contact-lens electrode (Cephalon, Nørresundby, Denmark) was placed on the cornea using a gel (Viscotears®; Novartis, Copenhagen, Denmark) as the contact fluid. A reference electrode was placed behind the ear. An infrared (IR) light emitter incorporated in the stimulation camera allowed continuous fundus monitoring. Responses were band-pass-filtered outside 10–300 Hz. Colour fundus photographs (Zeiss FF450 plusIR; Carl Zeiss, Jena, Germany) were obtained after completion of the mfERG

recordings. At 2 week evaluation, four pigs were euthanized and one pig was not fundus photographed due to technical difficulties; therefore, the spontaneous course could not be evaluated in these pigs.

The IR fundus picture was aligned with the corresponding fundus picture (Adobe Photoshop CC; Adobe®) to enable exact anatomical localization of each hexagon (Voss et al. 2007). Using the aligned pictures, mfERG recordings from detached areas within the visual streak (left eye) were averaged and compared to averaged recordings from corresponding areas in the right eye. This stabilized the variance by reducing the variation caused by the anaesthesia and the difference in amplitude between the animals. After control recordings were completed, an IV injection of 5 μg/kg of fentanyl (50 μg/ml; Hameln Pharmaceuticals GmbH, Hameln, Germany) was given and the treated eye was enucleated. Anaesthetized pigs were euthanized using an IV injection of 1 ml/kg of pentobarbital (200 mg/ml; Royal Veterinary and Agricultural University, Copenhagen, Denmark) and lidocaine hydrochloride (20 mg/ml; Glostrup Pharmacy, Glostrup Denmark).

Histology

The anterior segment and the lens were immediately removed from the enucleated eye, and the posterior segment was fixed in 4% paraformaldehyde. A segment containing the optic disc and the retinal detachment was identified, cut out and embedded in paraffin. Sections of 5 μm were taken through the lesion, and every other section was stained with haematoxylin and eosin (HE) and examined with a light microscope (Axioplan 2; Carl Zeiss). Digital images were obtained with an Axiocam HRC (Carl Zeiss).

All histologic evaluations were blinded, and sections were graded according to the appearance of the ganglion cell layer, the inner nuclear layer, the outer nuclear layer, the photoreceptor outer segments (OS) and the RPE, as previously described (Sorensen et al. 2017b). Each category was ordinally graded, where 0 = normal conditions, 1 = affected layer, 2 = degenerated layer and 3 = maximal damage with no retinal organization. The specimens were also examined for choroidal neovascularization (CNV), where 0 = not present and 1 = present.

Six unstained sections, containing the detached visual streak, from each animal were selected for immunohistochemical analysis. Immunohistochemical evaluation was performed on 5-μm sections using the antibodies against GFAP (Z0334; Dako, Glostrup, Denmark) to detect astrocytes and glia, vimentin (790-2917; Roche, Hvidovre, Denmark) to detect Müller cells and glia, BCl-2 (790-4464; Roche) to detect anti-apoptosis and Ki67 (790-4286; Roche) and cyclin D1 (790-4508; Roche) for cell proliferation (unspecific markers of cells that have entered cell division). All antibodies were used in line with the manufacturer's guidelines. Briefly, GFAP sections were pretreated with PT Link (Dako) using a high pH/low pH target-retrieval solution (DM828; Dako). Staining occurred on the Dako-Link 48 (Dako) utilizing the EnVision Flex+ detection kit (K8002; Dako). The primary GFAP antibody was diluted 1:8000 using antibody diluent (DM830; Dako) and was incubated with the specimens for 20 min. For vimentin, BCl-2, Ki67 and cyclin D1 sections, the staining took place on the Ventana Benchmark Ultra (Roche) using ultraView or OptiView detection kits (760–500 and 760–700, respectively). All sections were counterstained with haematoxylin.

The number of Müller cell processes in each specimen was counted in two representative sections in 100 μm of the transition zone between the inner plexiform layer and the inner nuclear layer. Cells in the ganglion cell layer were counted in three representative sections from each animal. Digital images were obtained, and a 500-μm zone was marked and magnified so that it filled the computer screen. Only cells with a clearly defined cell wall were counted using Fiji ImageJ 1.49. Retinal thickness was measured in detached retinas. For comparison, to examine whether a difference in retinal thickness could be explained by difference in retinal eccentricity, retinal thickness in relation to eccentricity was investigated in sections from a healthy eye between the optic nerve and 4000 μm superior.

Fluorescence immunohistochemistry

Evaluation of ganglion cells was performed with fluorescence immunohistochemistry staining with anti-NeuN antibody (#EPR12763 –Neuronal marker ab177487, Abcam, Cambridge, United Kingdom). Paraffin wax was removed by placing specimens in xylene (VWR chemicals, Søborg, Denmark) for 5 min. Subsequently, specimens were rehydrated in 99% ethanol (Region Hovedstadens Apotek, Herlev, Denmark) for 5 min and 95% ethanol (Region Hovedstadens Apotek, Herlev, Denmark) and 70% ethanol for 2 min, respectively. The rehydrated sections were rinsed in distilled H_2O (Region Hovedstadens Apotek, Herlev, Denmark) and 0.1M PBS (Life Technologies, Thermo Fischer Scientific, Paisley, UK) containing 0.25% Triton X-100 (=PBST) (Sigma-Aldrich, Brøndbyvester, Denmark). Heat-mediated (95–98°C) antigen retrieval was performed in 1 mM EDTA buffer pH 8.0 for 15 min and specimens subsequently rinsed in 4°C PBST. The rinsed specimens were exposed to primary antibody (NeuN) diluted in 0.1M PBST and 1% bovine serum albumin (BSA) (Sigma-Aldrich, Brøndbyvester, Denmark) in a moist chamber at 4°C for 16–18 hr. Subsequently, sections were rinsed in PBST and incubated with PBST and 1% BSA with appropriate FITC secondary antibodies (1:100 dilution; Larodan, Solna, Sweden) for 1 hr at room temperature. Finally, specimens were rinsed in PBST and mounted with Vectashield+DAPI (Vector Laboratories, Burlingame, USA).

Data and statistical analyses

VERIS software was used to extract the amplitudes and implicit times from the mfERG recordings. The visual streak was identified on the aligned photography as previously described (Sorensen et al. 2017a) and defined as a four-hexagon tall band, stretching horizontally one hexagon above the optic nerve head. A detached area inside the visual streak that was the size of 10 hexagons was chosen for analysis. The ratio of the major mfERG amplitudes (the direct response (DR) and the induced component (IC)) measured from peak to trough (Sorensen et al. 2017a) was analysed using mixed models in SAS Enterprise Guide 7.1® (SAS Institute Inc., Cary, NC, USA). Means and 95% confidence intervals (CI) of the amplitude ratios (right/left eye) were calculated. $p < 0.05$ was considered significant.

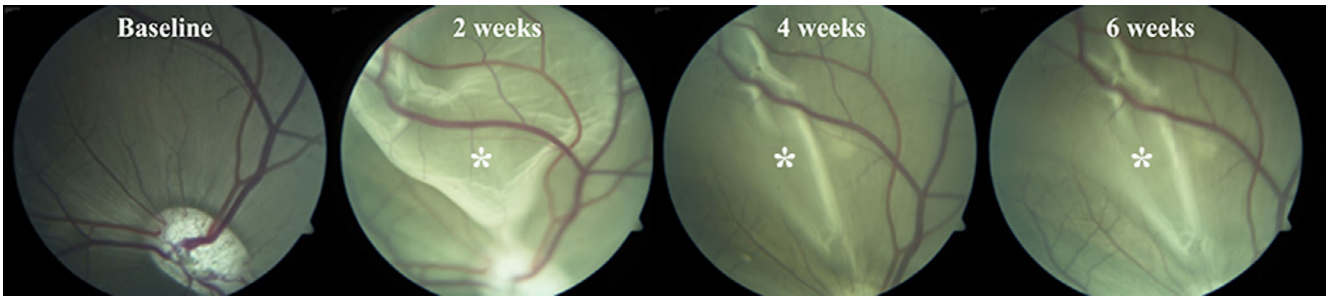

Fig. 1. Fundus photographs of the spontaneous partial reattachment of a rhegmatogenous-like retinal detachment in the porcine eye. The pictures show fundus photographs from the same pig at four different evaluation times. At baseline, prior to surgery, the retina is healthy and attached. At 2 weeks after surgery, a large bullous retinal detachment can be seen. At 4 weeks after surgery, the retina has partially reattached and the picture is similar at 6 weeks after surgery. *Retinal detachment.

Results

A total of 11 out of 12 pigs developed a rhegmatogenous-like retinal detachment (Fig. 1). Rhegmatogenous-like retinal detachments were characterized by loss of retinal tension (Fig. 1). Between weeks 2 and 4, the rhegmatogenous-like retinal detachments spontaneously and partially reattached in six out of six pigs with fundus photographs at the two evaluation time points (Fig. 1).

Retinal function

Multifocal electroretinogram (MfERG) amplitudes recorded from detached areas were significantly reduced compared to mfERG amplitudes recorded at baseline (Figs 2 and 3). The mfERG topography was evaluated, and no difference was observed between reattached and detached areas (Fig. 2). The DR ratio (treated/untreated eye) decreased after 2 weeks (M = −0.83 nV/deg^2, confidence limits (CL) = (−1.09, −0.56) nV/deg^2, $p < 0.0001$), and this decrease persisted after 4 weeks (M = −0.95 nV/deg^2, CL = (−1.25, −0.64) nV/deg^2, $p < 0.0001$) and 6 weeks (M = −0.99 nV/deg^2, CL = −1.38, −0.61, $p < 0.0001$) nV/deg^2. The IC ratio (treated/untreated eye) was also significantly decreased after 2 weeks compared to baseline (M = −1.26 nV/deg^2, CL = (−1.69, −0.83) nV/deg^2, $p < 0.0001$). As seen for the DR, the IC decrease also persisted after 4 weeks (M = −1.21 nV/deg^2, CL = (−1.72, −0.71) nV/deg^2, $p = 0.0001$) and 6 weeks (M = −1.44 nV/deg^2, CL = (−2.10, −0.79) nV/deg^2, $p = 0.0003$). No significant differences were observed between 2, 4 and 6 weeks for either the DR or IC ratio (Fig. 3).

Retinal morphology

Loss of photoreceptor OS (grade 2) was seen in HE-stained specimens in all eyes (Figs 4 and 5). Defragmentation of the inner nuclear layer (grade 1) was seen in 10 of the 11 evaluated eyes (Fig. 6). In the histological sections, there were no signs of oedema; there were no swelling of the retina, no eosinophil material in the subretinal space and no intraretinal cysts.

The RPE was hypopigmented in the debrided area in 10 of the 11 eyes and double or multilayered in 3 of the 11 eyes (grade 1). None of the eyes had areas devoid of RPE. The mean number of cells in the ganglion cell layer/500 µm was 44.73 cells (CL = 39.45, 50.01). None of the eyes had affected outer nuclear layer (grade 0) or CNV (grade 0).

After detachment, the mean retinal thickness decreased by 27.9%, from mean thickness of 280 µm at baseline to mean thickness of 202 µm at 6 weeks. The decrease was primarily located in the inner plexiform layer, the ganglion cell layer and the nerve fibre layer (Figs 4 and 5).

In the healthy eye, retinal thickness in relation to eccentricity from the optic nerve decreased by 12% between the optic nerve and 4000 µm superior. The mean difference in retinal thickness between the temporal and nasal side in a healthy histological section was 10.5%.

Staining for vimentin and GFAP increased with time following detachment (Fig. 5). The mean number of Müller cell processes/100 µm was 15.5 (baseline), 15.1 (2 weeks), 15.3 (4 weeks) and 15.2 (6 weeks), respectively. Unspecific Ki67 staining was observed in the entire porcine retina. Positive cytoplasmic staining of cyclin D1 was shown in the ganglion cell layer (Fig. 5). No BCl-2-positive cells were identified.

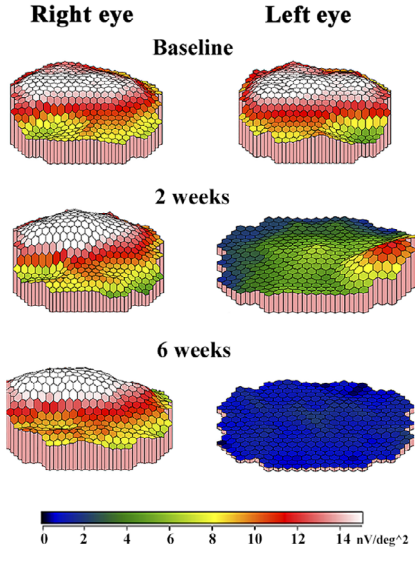

Fig. 2. MfERG amplitude topography from the same pig at different evaluation times. At baseline, before surgery, the retina is attached in both eyes. The visual streak is a ridge in white and red, and the optic disc is a depression in green in both eyes. In the healthy right eye, where the retina remains attached, the mfERG topography is similar at all evaluation times. In the left eye, which underwent surgical induction of a rhegmatogenous-like retinal detachment after baseline recordings, the mfERG topography decreases. After 2 weeks, the mfERG response from the visual streak is seen in green. After 6 weeks, the blue colours show that there is no mfERG response in the left eye.

Fluorescence immunohistochemical staining for ganglion cells showed that ganglion cells had lost their nucleus and nucleolus 2 weeks after detachment (Fig. 7).

Discussion

This study successfully established, for the first time in an *in vivo* model, a retinal

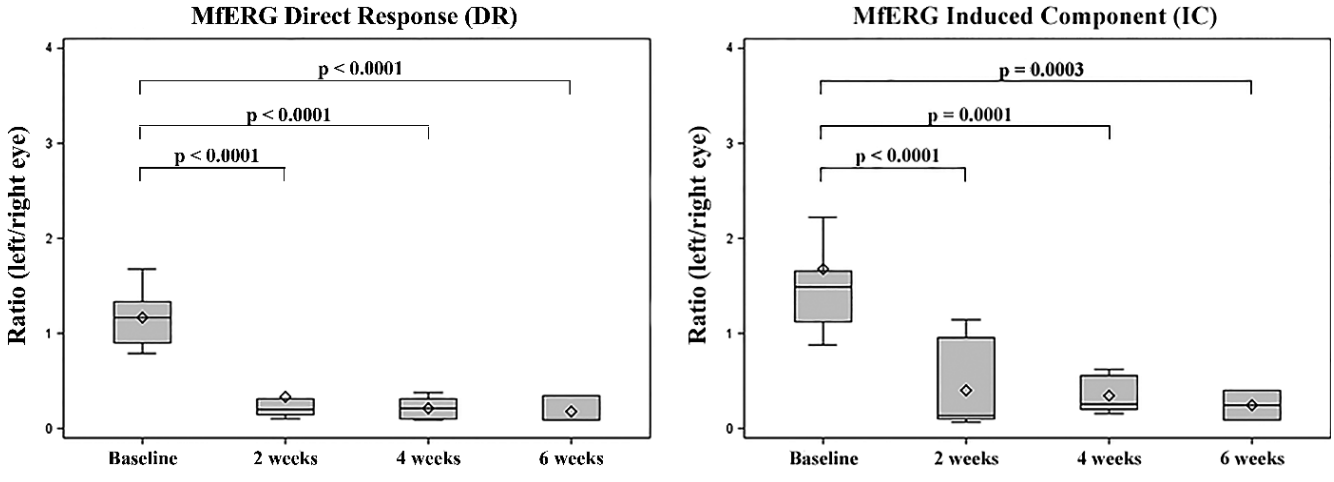

Fig. 3. Box plots of mfERG amplitudes before (baseline) and after rhegmatogenous-like retinal detachment. Although the retinas partially reattached, there was a significant and lasting decrease in retinal function. The rhombus within the box represents the median, and the line within the box represents the average.

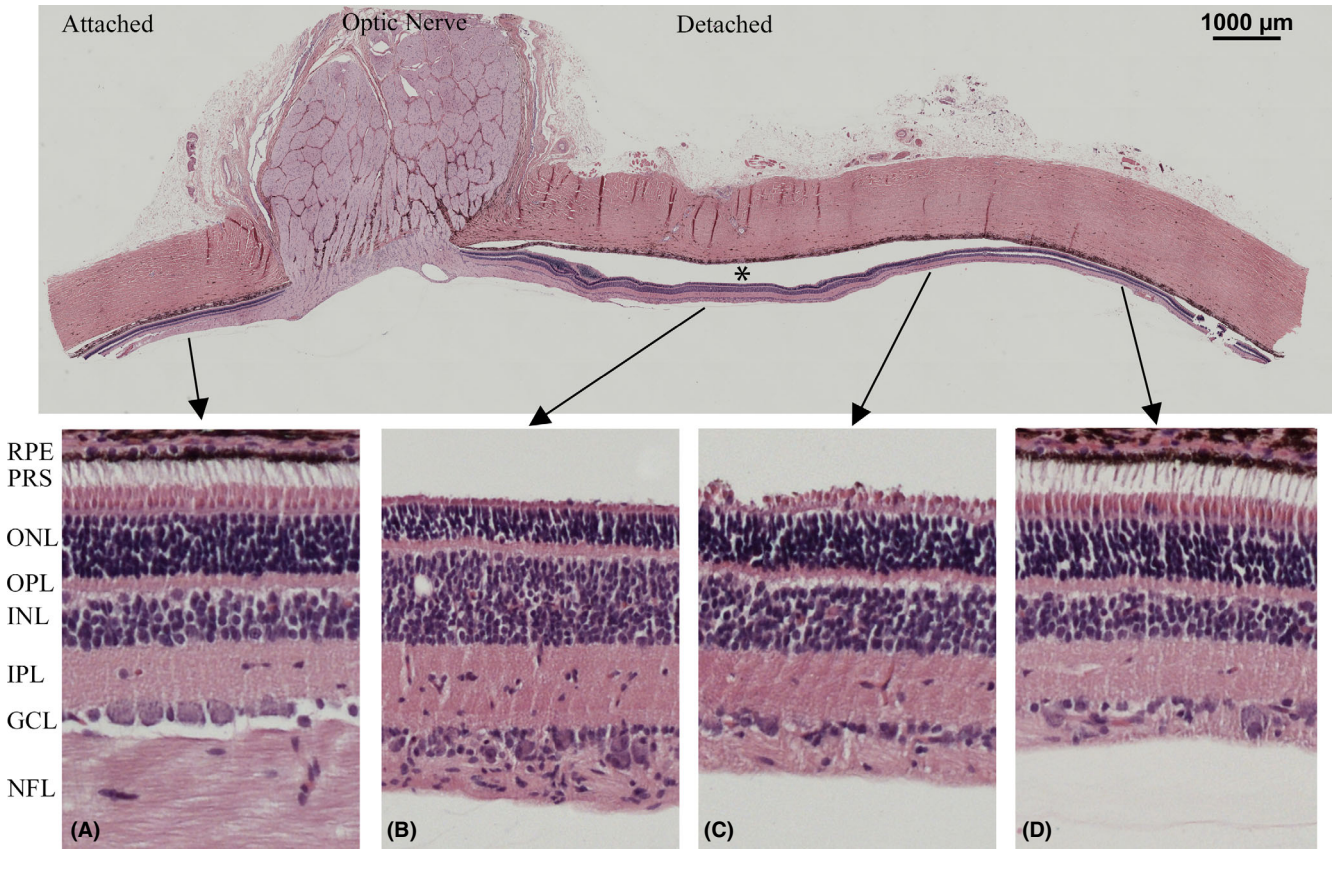

Fig. 4. Retinal micrograph of HE-stained section with magnification of attached and detached areas for direct comparison. Shortening of photoreceptor outersegments, increased cellularity of the inner nuclear layer and ganglion cell layer, decreased thickness of nerve fibre layer are seen in detached areas compared to attached areas. *Detached retina.

detachment with loss of retinal tension and permanent loss of visual function. The model makes it possible to study the time-related disease progression and test new treatment modalities for rhegmatogenous retinal detachment.

In the present study, the retinas detached and retinal tension was lost after extensive RPE removal, and the retinal function measured with mfERG was significantly decreased. The findings in the present study differ from our earlier porcine studies. We have previously found that retinal structure and function is preserved despite prolonged shallow detachment (Sorensen et al. 2012) and a large distance between RPE and photoreceptors (Sorensen et al. 2017b). We can therefore conclude that, at least in the porcine model, separation of photoreceptors and RPE is well tolerated as long as retinal tension is preserved.

Previous RRD models have induced retinal detachments by subretinal

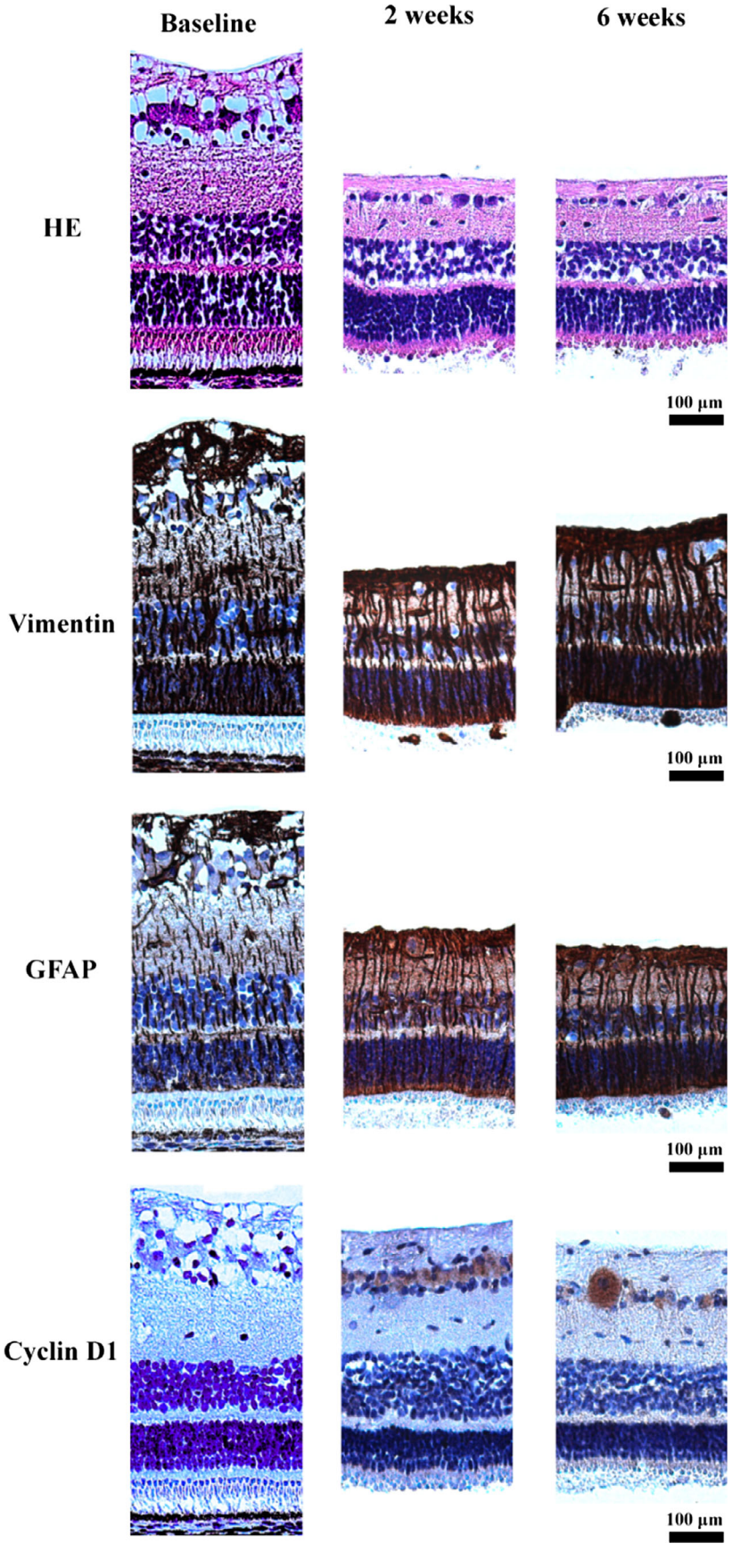

Fig. 5. Micrographs of rhegmatogenous-like detached porcine retinas at different time points. Loss of photoreceptor OS was seen in HE-stained specimens. Müller cells are seen in brown colours in the vimentin- and GFAP-stained specimens. Proliferating cells are seen in brown in the cyclin D1-stained specimens. Overall, the thickness of the inner nuclear layer, the inner plexiform layer and the nerve fibre layer decreased with time after detachment. The distance from the optic nerve (eccentricity) was comparable between the retinal sections.

injection of fluid (Anderson et al. 1983, 1986; Erickson et al. 1983; Guerin et al. 1989, 1990, 1993; Fisher et al. 1991, 2001, 2005; Cook et al. 1995; Lewis et al. 1998, 2002, 2005; Jacobs et al. 2002; Lewis & Fisher 2003; Linberg et al. 2009; Mandal et al. 2011; Sorensen et al. 2012, 2017b). These models have increased our understanding of one of the main characteristics of retinal detachment; loss of contact between photoreceptors and RPE. However, the significance of retinal tension has not previously been explored *in vivo*.

In the previous models, the fluid injected into the subretinal space to produce the detachments increased the retinal tension. *In vitro*, Taylor et al. (2013) have shown that retinal architecture is preserved, neuronal cell survival is increased, and there is no gliosis in stretched retinas. This protective response induced by increased retinal tension could explain sustained retinal function despite detachment in our previous porcine models (Sorensen et al. 2012, 2017b). Conversely, in human rhegmatogenous retinal detachment and in the present RPE debridement model with loss of retinal tension, retinal function decreases.

Two to six weeks after debridement, areas with hypopigmented RPE was observed, but no areas were devoid of RPE. This is in accordance with earlier findings where denuded Bruch's membrane within 1 week is repopulated by hypopigmented RPE proliferating from the periphery (Kiilgaard et al. 2007; Sorensen et al. 2013). For detailed pictures of these hypopigmented RPE cells as well as electron-microscopic photographs of denuded Bruch's membrane, we refer to these previously published papers (Kiilgaard et al. 2007; Sorensen et al. 2013).

The size of the RPE debridement seems to determine the chance of surgically induced retinal detachment. In a previous study, the retina remained attached at all times after a smaller RPE debridement (Sorensen et al. 2013). Contrary, after the extensive RPE debridement in the present study, the retinas detached. In accordance with this

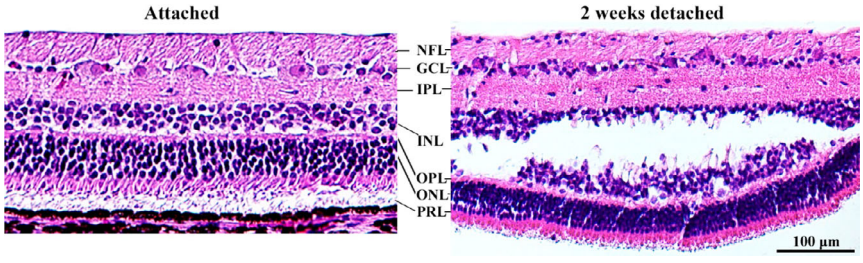

Fig. 6. Micrographs of HE-stained retinal sections in an attached retina and 2 weeks after detachment. Compared to the attached retina, increased cellularity is seen in the GCL layer after detachment. Defragmentation of the INL is representative for what is seen in smaller or larger areas in all specimens at 2–6 weeks after rhegmatogenous-like retinal detachment. This defragmentation might represent an artefact. However, we have not observed such a defragmentation in previous porcine retinal detachment models [1, 2]. GCL = ganglion cell layer, INL = inner nuclear layer, IPL = inner plexiform layer, NFL = nerve fibre layer, ONL = outer nuclear layer, OPL = outer plexiform layer, PRL = photoreceptor layer.

hypothesis, spontaneous retinal detachments have been observed after massive RPE damage by systemic administration of iodate (Davson & Hollingsworth 1972; Negi & Marmor 1983).

In the present study, retinal function decreased although the retinas spontaneously and partially reattached. The partial reattachment could be explained by the return of RPE to the debrided area (Kiilgaard et al. 2007; Sorensen et al. 2013) and thereby reestablishment of the adhesive force (Marmor & Maack 1982; Negi & Marmor 1983; Marmor 1990). Another possibility is that the return of RPE restores a barrier that prevents fluid from entering the subretinal space from the choroid, pushing the retina away (Marmor 1979, 1988).

It could be speculated whether the permanent loss of retinal function was caused by the RPE debridement or the large retinotomy. However, in a previous study retinal function returned to normal after a large retinotomy in combination with a smaller RPE debridement (Sorensen et al. 2013). In the previous study, the retinas remained attached at all times. In the present study, it is therefore likely that it was the detachment (and not the retinotomy or the debridement) that caused the decrease in retinal function measured with mfERG.

It should be considered whether the decreased mfERG amplitudes in the present model represent a true loss of retinal function. In theory, the anteriorly shifted retina being out of focus could cause the decreased amplitudes. However, we have previously found normal mfERG amplitudes despite ongoing retinal detachment after subretinal injection in the porcine model (Sorensen et al. 2012). Furthermore, a human study found that the P1 amplitude, which is recommended for evaluating retinal function in pigs (Voss et al. 2007), remained stable regardless of focus (Vrabec et al. 2004). In addition, no difference in mfERG topography was observed between detached and reattached area in the present study. It is therefore probable that the decreased mfERG amplitudes in the present model represent a true decrease in retinal function.

Retinal function measured by mfERG consists of responses from both outer and inner retina (Hood 2000; Shimada et al. 2005). Histologically, in the present study, the induced changes in the in the outer retina were surprisingly modest and limited to shortening of outer segments. Studies in small-animal-models have found that the earliest retinal change after separation of the photoreceptors from the RPE is outer segment degeneration (Fisher et al. 2005; Linberg et al. 2009).

However, even such a modest change would induce loss of outer retinal mfERG signal. In the present model, the cells in the outer nuclear layer remained intact and regeneration of outer segments and thereby restoration of outer retinal signal could therefore be possible. The permanent loss of visual function must therefore be due to loss of function elsewhere.

Death of retinal ganglion cells could explain the lasting loss of retinal function. In the fluorescence immunohistochemical staining, loss of ganglion cell nucleus and nucleolus was observed at all control times after detachment. This is a sign of ganglion cell death, from which the cells will not regenerate and loss of retinal function is thereby permanent.

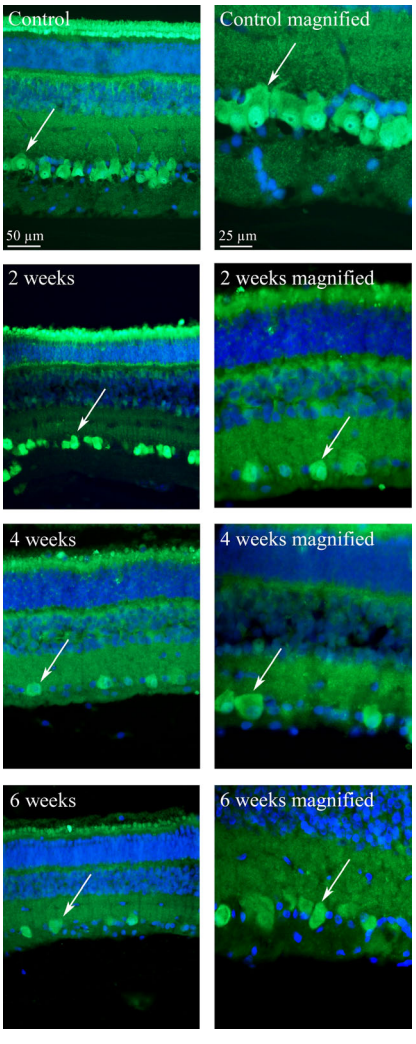

Fig. 7. Retinal micrographs stained with NeuN for ganglion cells (fluorescent green) and with DAPI for the nucleus of other cells (blue). In the controls (healthy retina), the retinal ganglion cells (arrow) are clearly defined with a distinct nucleus (bright green) and nucleolus (black spot inside the nucleus). At all time points, after detachment the ganglion cells (arrows) are "empty" with no nucleus or nucleolus Sorensen et al. 2012, 2017b.

Despite death of ganglion cells, increased cellularity in the retinal ganglion cell layer was observed. In the visual streak, an average of 41 cells/500 µm was identified compared to the expected 25 ganglion cells/500 µm in healthy retinas (Kyhn et al. 2009). Increased cellularity was accompanied by cytoplasmic staining with cyclin D1, which has been shown to prevent apoptosis in neuronal cells (Sumrejkanchanakij et al. 2003; Alao et al. 2006).

The cells in the ganglion cell layer did not stain with the fluorescent immunohistochemical staining for ganglion cells. No nuclear staining was

observed for the proliferative markers Ki67 and cyclin D1 (unspecific markers for cell-division cycle). The lack of staining shows that increased proliferation of retinal cells cannot explain the increased cellularity. Morphologically, the cells do not look like lymphocytes and the identity of the cells remains unknown. Developing specific staining for the unknown porcine cells is beyond the scope of this paper.

Furthermore, unspecific reactive changes in glial cells were also identified, as demonstrated by increased GFAP and vimentin staining and hypertrophy of Müller cell processes. These findings have been described as stress responses after retinal detachment in other species and proposed to be involved in the formation of glial scars (Lewis & Fisher 2003).

Retinal thickness decreased after retinal detachment. Retinal thickness in relation to eccentricity was evaluated in healthy specimens to examine whether our finding could be caused by difference in eccentricity between compared specimens. Our results showed that retinal thickness truly decreased after retinal detachment.

The defragmentation observed in the inner nuclear layer (INL) might represent an artefact. However, we have not observed such a defragmentation in previous porcine retinal detachment models (Sorensen et al. 2012, 2017b). Furthermore, defragmentation only occurred in detached areas and not attached areas in the same specimens. We cannot rule out that the finding could be artifactual, but it would be peculiar if an artefact was only seen in INL and no other layers.

It is possible that increased retinal tension in serous detachments and our previous porcine models (Sorensen et al. 2013, 2017b) may activate mechanoreceptors and generate a neuroprotective response that sustains retinal function. This theory needs to be investigated in future studies.

Conclusions

Retinal detachment with loss of retinal tension induces ganglion cell death and permanent loss of retinal function in the porcine model. For the first time in a large mammal, this model enables new therapeutic interventions to be tested with the aim of preventing permanent loss of vision after retinal detachment. The model might deliver new perspectives and answers to the very different outcomes between a serous retinal detachment (retinal tension is maintained) and a rhegmatogenous retinal detachment (retinal tension is lost).

References

Alao JP, Gamble SC, Stavropoulou AV, Pomeranz KM, Lam EW, Coombes RC & Vigushin DM (2006): The cyclin D1 proto-oncogene is sequestered in the cytoplasm of mammalian cancer cell lines. Mol Cancer **5**: 7.

Anderson DH, Stern WH, Fisher SK, Erickson PA & Borgula GA (1983): Retinal detachment in the cat: the pigment epithelial-photoreceptor interface. Invest Ophthalmol Vis Sci **24**: 906–926.

Anderson DH, Guerin CJ, Erickson PA, Stern WH & Fisher SK (1986): Morphological recovery in the reattached retina. Invest Ophthalmol Vis Sci **27**: 168–183.

Cook B, Lewis GP, Fisher SK & Adler R (1995): Apoptotic photoreceptor degeneration in experimental retinal detachment. Invest Ophthalmol Vis Sci **36**: 990–996.

Davson H & Hollingsworth JR (1972): The effects of iodate on the blood-vitreous barrier. Exp Eye Res **14**: 21–28.

Erickson PA, Fisher SK, Anderson DH, Stern WH & Borgula GA (1983): Retinal detachment in the cat: the outer nuclear and outer plexiform layers. Invest Ophthalmol Vis Sci **24**: 927–942.

Fisher SK, Erickson PA, Lewis GP & Anderson DH (1991): Intraretinal proliferation induced by retinal detachment. Invest Ophthalmol Vis Sci **32**: 1739–1748.

Fisher SK, Stone J, Rex TS, Linberg KA & Lewis GP (2001): Experimental retinal detachment: a paradigm for understanding the effects of induced photoreceptor degeneration. Prog Brain Res **131**: 679–698.

Fisher SK, Lewis GP, Linberg KA & Verardo MR (2005): Cellular remodeling in mammalian retina: results from studies of experimental retinal detachment. Prog Retin Eye Res **24**: 395–431.

Guerin CJ, Anderson DH, Fariss RN & Fisher SK (1989): Retinal reattachment of the primate macula. Photoreceptor recovery after short-term detachment. Invest Ophthalmol Vis Sci **30**: 1708–1725.

Guerin CJ, Anderson DH & Fisher SK (1990): Changes in intermediate filament immunolabeling occur in response to retinal detachment and reattachment in primates. Invest Ophthalmol Vis Sci **31**: 1474–1482.

Guerin CJ, Lewis GP, Fisher SK & Anderson DH (1993): Recovery of photoreceptor outer segment length and analysis of membrane assembly rates in regenerating primate photoreceptor outer segments. Invest Ophthalmol Vis Sci **34**: 175–183.

Hamann S (2002): Molecular mechanisms of water transport in the eye. Int Rev Cytol **215**: 395–431.

Hood DC (2000): Assessing retinal function with the multifocal technique. Prog Retin Eye Res **19**: 607–646.

Jacobs GH, Calderone JB, Sakai T, Lewis GP & Fisher SK (2002): An animal model for studying cone function in retinal detachment. Doc Ophthalmol **104**: 119–132.

Kiilgaard JF, Prause JU, Prause M, Scherfig E, Nissen MH & la Cour M (2007): Subretinal posterior pole injury induces selective proliferation of RPE cells in the periphery in *in vivo* studies in pigs. Invest Ophthalmol Vis Sci **48**: 355–360.

Kyhn MV, Klassen H, Johansson UE et al. (2009): Delayed administration of glial cell line-derived neurotrophic factor (GDNF) protects retinal ganglion cells in a pig model of acute retinal ischemia. Exp Eye Res **89**: 1012–1020.

Lewis GP & Fisher SK (2003): Up-regulation of glial fibrillary acidic protein in response to retinal injury: its potential role in glial remodeling and a comparison to vimentin expression. Int Rev Cytol **230**: 263–290.

Lewis GP, Linberg KA & Fisher SK (1998): Neurite outgrowth from bipolar and horizontal cells after experimental retinal detachment. Invest Ophthalmol Vis Sci **39**: 424–434.

Lewis GP, Charteris DG, Sethi CS & Fisher SK (2002): Animal models of retinal detachment and reattachment: identifying cellular events that may affect visual recovery. Eye **16**: 375–387.

Lewis GP, Sethi CS, Carter KM, Charteris DG & Fisher SK (2005): Microglial cell activation following retinal detachment: a comparison between species. Mol Vis **11**: 491–500.

Linberg KA, Lewis GP & Fisher SK (2009): Retraction and remodeling of rod spherules are early events following experimental retinal detachment: an ultrastructural study using serial sections. Mol Vis **15**: 10–25.

Mandal N, Lewis GP, Fisher SK, Heegaard S, Prause JU, la Cour M, Vorum H & Honore B (2011): Protein changes in the retina following experimental retinal detachment in rabbits. Mol Vis **17**: 2634–2648.

Marmor MF (1979): Retinal detachment from hyperosmotic intravitreal injection. Invest Ophthalmol Vis Sci **18**: 1237–1244.

Marmor MF (1988): New hypotheses on the pathogenesis and treatment of serous retinal detachment. Graefes Arch Clin Exp Ophthalmol **226**: 548–552.

Marmor MF (1990): Control of subretinal fluid: experimental and clinical studies. Eye, **4**(Pt 2): 340–344.

Marmor MF & Maack T (1982): Enhancement of retinal adhesion and subretinal fluid resorption by acetazolamide. Invest Ophthalmol Vis Sci **23**: 121–124.

Negi A & Marmor MF (1983): The resorption of subretinal fluid after diffuse damage to the retinal pigment epithelium. Invest Ophthalmol Vis Sci **24**: 1475–1479.

Nicholson B, Noble J, Forooghian F & Meyerle C (2013): Central serous chorioretinopathy: update on pathophysiology and treatment. Surv Ophthalmol **58**: 103–126.

Pastor JC, Rojas J, Pastor-Idoate S, Di Lauro S, Gonzalez-Buendia L & Delgado-Tirado S (2016): Proliferative vitreoretinopathy: a new concept of disease pathogenesis and practical consequences. Prog Retin Eye Res **51**: 125–155.

Shimada Y, Bearse MA, Jr & Sutter EE (2005): Multifocal electroretinograms combined with periodic flashes: direct responses and induced components. Graefes Arch Clin Exp Ophthalmol **243**: 132–141.

Sorensen NF, Ejstrup R, Svahn TF, Sander B, Kiilgaard J & la Cour M (2012): The effect of subretinal viscoelastics on the porcine retinal function. Graefes Arch Clin Exp Ophthalmol **250**: 79–86.

Sorensen NB, Lassota N, Kyhn MV, Prause JU, Qvortrup K, la Cour M & Kiilgaard J (2013): Functional recovery after experimental RPE debridement, mfERG studies in a porcine model. Graefes Arch Clin Exp Ophthalmol **251**: 2319–2325.

Sorensen NB, Christiansen AT, Kjaer TW, Klemp K, la Cour M & Kiilgaard JF (2017a): Time-dependent decline in multifocal electroretinogram requires faster recording procedures in anesthetized pigs. Transl Vis Sci Technol **6**: 6.

Sorensen NB, Klemp K, Kjaer TW, Heegaard S, la Cour M & Kiilgaard JF (2017b): Repeated subretinal surgery and removal of subretinal decalin is well tolerated - evidence from a porcine model. Graefes Arch Clin Exp Ophthalmol **255**(9): 1749–1756.

Sparrow JR, Hicks D & Hamel CP (2010): The retinal pigment epithelium in health and disease. Curr Mol Med **10**: 802–823.

Strauss O (2005): The retinal pigment epithelium in visual function. Physiol Rev **85**: 845–881.

Sumrejkanchanakij P, Tamamori-Adachi M, Matsunaga Y, Eto K & Ikeda MA (2003): Role of cyclin D1 cytoplasmic sequestration in the survival of postmitotic neurons. Oncogene **22**: 8723–8730.

Taylor L, Moran D, Arner K, Warrant E & Ghosh F (2013): Stretch to see: lateral tension strongly determines cell survival in long-term cultures of adult porcine retina. Invest Ophthalmol Vis Sci **54**: 1845–1856.

Voss Kyhn M, Kiilgaard JF, Lopez AG, Scherfig E, Prause JU & la Cour M (2007): The multifocal electroretinogram (mfERG) in the pig. Acta Ophthalmol Scand **85**: 438–444.

Vrabec TR, Affel EL, Gaughan JP, Foroozan R, Tennant MT, Klancnik JM, Jr, Jordan CS & Savino PJ (2004): Voluntary suppression of the multifocal electroretinogram. Ophthalmology **111**: 169–176.

Received on December 7th, 2017.
Accepted on June 15th, 2019.

Correspondence:
Nina Buus Sørensen
Department of Ophthalmology
Copenhagen University Hospital
Rigshospitalet
Copenhagen
Denmark
Email: nina.buus.soerensen@regionh.dk

This manuscript has been professionally proofread.